Available online at BCREC website: https://bcrec.id

Bulletin of Chemical Reaction Engineering & Catalysis, 18 (3) 2023, 353-361

Short Communications

Synthesis, Structural Characterization and Photocatalytic CO_2 Reduction Activity of a New Gd(III) Coordination Polymer with 6-Phenylpyridine-2-carboxylic acid and 4,4'-Bipyridine Ligands

Xi-Shi Tai[1], Yuan-Fang Wang[1], Li-Hua Wang[2], Xi-Hai Yan[1,*]

[1]College of Chemistry and Chemical Engineering, Weifang University, Weifang 261061, P. R. China.
[2]College of Biology and Oceanography, Weifang University, Weifang 261061, P. R. China.

Received: 20th July 2023; Revised: 9th August 2023; Accepted: 9th August 2023
Available online: 13rd August 2023; Published regularly: October 2023

Abstract

A new Gd(III) coordination polymer, $\{[Gd(L_1)_3(H_2O)_2]\cdot L_2\}_n$ (**1**) (HL_1 = 6-phenylpyridine-2-carboxylic acid, L_2 = 4,4'-bipyridine) was synthesized using 6-phenylpyridine-2-carboxylic acid, 4,4'-bipyridine, NaOH and $GdCl_3\cdot 6H_2O$. The structure of Gd(III) coordination polymer has been characterized by IR and X-ray single crystal diffraction. The result of single crystal analysis indicates that fundamental unit of Gd(III) coordination polymer contains one Gd(III) ion, three L_1 ligands, two coordinated water molecules and one uncoordinated 4,4'-bipyridine. In **1**, the Gd(III) ion is eight-coordinated and surrounded by six O atoms from three L_1 ligands and two O atoms from two coordinated water molecules, respectively. The complex **1** exhibits 1D chained structure by the bridging interactions of two carboxyl-oxygen atoms and O–H···N hydrogen bonds interactions. The 1D chains are further connected by π-π stacking interactions to form 3D network architecture. The photocatalytic CO_2 reduction activity of complex **1** has also been investigated. The complex **1** exhibits good CO_2 reduction activity. With the increase of time, the yield of CO from 18.2 μmol/g in the first hour to 60.3 μmol/g in the third hour. And the CO selectivity has reached 100%.

Keywords: 6-Phenylpyridine-2-carboxylic acid; 4,4'-bipyridine; Gd(III) coordination polymer; Synthesis; Structural Characterization; Photocatalytic CO_2 reduction

How to Cite: X.S. Tai, Y.F. Wang, L.H. Wang, X.H. Yan (2023). Synthesis, Structural Characterization and Photocatalytic CO2 Reduction Activity of a New Gd(III) Coordination Polymer with 6-Phenylpyridine-2-carboxylic acid and 4,4'-Bipyridine Ligands. *Bulletin of Chemical Reaction Engineering & Catalysis*, 18(3), 353-361 (doi: 10.9767/bcrec.19540)

Permalink/DOI: https://doi.org/10.9767/bcrec.19540

1. Introduction

In recent years, rare earth coordination polymers constructed by organic carboxylate ligands have aroused the wide interest of chemists because they have shown excellent properties in photoluminescence [1–3], magnetic properties [4–6], anticancer drug [7,8], CO_2 adsorption [9]. And they also showed excellent catalytic activities, such as photocatalytic and electrocatalytic activity include the oxygen reduction reaction (ORR), hydrogen evolution reaction (HER), oxygen evolution reaction (OER), CO_2 reduction reaction (CO_2RR) [10], CO_2 cycloaddition reaction [11], ring-opening polymerizations [12], stereoselective polymerization for aromatic polar vinyl monomerserizations [13], polymerization of dienes, vinyl monomers, and epsiloncaprolactone [14], polymerization of cyclic esters [15]. With the rapid development of human activities, a large amount of CO_2 is produced, and CO_2 will

* Corresponding Author.
Email: taixs@wfu.edu.cn (X.H. Yan);
Telp: +86-536-8785286, Fax: +86-536-8785286

cause greenhouse effect, climate change, soil acidification, increased disease and insect pests, and other problems, so the reduction of CO_2 into high value-added energy-containing fuels is an important research work [16]. However, recent studies on catalysts for photocatalytic reduction of CO_2 have focused on transition metal complexes because of the difficulty of obtaining single crystals of rare earth metal complexes [17–22]. In general, there are relatively few studies on photocatalytic reduction of CO_2 as a catalytic catalyst by rare earth coordination polymers [10].

6-Phenylpyridine-2-carboxylic acid can be coordinated to metal ions in a bidentate or tridentate coordination modes, and we have synthesized and characterized some of its complexes with Zn(II), Co(II), Pb(II), Cu(II), Ni(II), Cd(II) and Mn(II) ions [23–31]. So far, there are no reports of 6-phenylpyridine-2-carboxylic acid complexes with rare earth. To further investigate the structure and properties of 6-phenylpyridine-2-carboxylic acid complexes with rare earth, in this work, we have synthesized a new Gd(III) coordination polymer, $\{[Gd(L_1)_3(H_2O)_2]\cdot L_2\}_n$ (**1**) (HL_1 = 6-phenylpyridine-2-carboxylic acid, L_2 = 4,4'-bipyridine) was synthesized using 6-phenylpyridine-2-carboxylic acid, 4,4'-bipyridine, NaOH and $GdCl_3\cdot 6H_2O$. The structure of complex **1** was determined by single crystal X-ray diffraction. The photocatalytic CO_2 reduction activity of complex **1** has also been investigated.

2. Materials and Methods

2.1 Materials and Measurements

6-Phenylpyridine-2-carboxylic acid (A. R.) and 4,4'-bipyridine (A. R.) was purchased from Jilin Chinese Academy of Sciences-Yanshen Technology Co., Ltd.. $GdCl_3\cdot 6H_2O$ (A. R.) and NaOH (A. R.) were purchased from Jinan Henghua Sci. & Tec. Co., Ltd.. IR spectra were obtained with a KBr pellet on a FTIR-850 spectrometer (range ~4000–400 cm^{-1}) (Tianjin Gangdong Sci. & Tech. Co., Ltd, Tianjin, China). Crystal data of complex **1** were obtained with a Bruker Smart CCD diffractometer (Bruker, Billerica, MA, USA). The reactor of photocatalytic CO_2 reduction was sealed and irradiated using a 300 W Xe arc lamp (Beijing

Table 1. The important crystal data for $\{[Gd(L_1)_3(H_2O)_2]\cdot L_2\}_n$ (**1**).

Empirical formula	$C_{41}H_{32}N_4O_8Gd$
Formula weight	865.95
Temperature/K	250.00(10)
Crystal size/mm^3	0.13 × 0.10 × 0.08
Crystal system	monoclinic
Space group	$P2_1/n$
a/Å	18.1899(15)
b/Å	10.5157(6)
c/Å	21.2809(17)
α/°	90
β/°	104.616(8)
γ/°	90
Volume/$Å^3$	3938.9(5)
Z	4
ρ_{calc}, mg/mm^3	1.460
μ/mm^{-1}	1.740
S	1.044
F(000)	1736
Index ranges	$-21 \le h \le 21$, $-12 \le k \le 12$, $-25 \le l \le 17$
Reflections collected	18818
2θ/°	4.35-49.998
Independent reflections	6936 [R(int) = 0.0488]
Data/restraints/parameters	6936/1/493
Goodness-of-fit on F^2	1.044
Refinement method	Full-matrix least-squares on F^2
Final R indexes [I>=2σ (I)]	R_1 = 0.0344, wR_2 = 0.0590
Final R indexes [all data]	R_1 = 0.0489, wR_2 = 0.0660

Trusttech Co., Ltd (PLS-SXE300)). The gas products have been achieved every hour and performed the detection using a gas chromatograph (GC-6890, Purkinje General instrument Co., Ltd., Beijing, China) equipped with Porapak Q column with FID detector.

2.2 Synthesis of $\{[Gd(L_1)_3(H_2O)_2]\cdot L_2\}_n$ (**1**)

0.3716 g (1.0 mmol) $GdCl_3\cdot 6H_2O$ was added a solution of 30 mL water-ethanol (v:v = 1:2) containing 0.1992 g (1.0 mmol) 6-phenylpyridine-2-carboxylic acid, 0.1562 g (1.0 mmol) 4,4'-bipyridine, and 0.040 g (1.0 mmol) NaOH with stirring. The solution was stirred for 5 h at 75 °C and cooled to room temperature. The crystals of $\{[Gd(L_1)_3(H_2O)_2]\cdot L_2\}_n$ (**1**) were received after the filtrate was slowly volatilized for 20 days at room temperature.

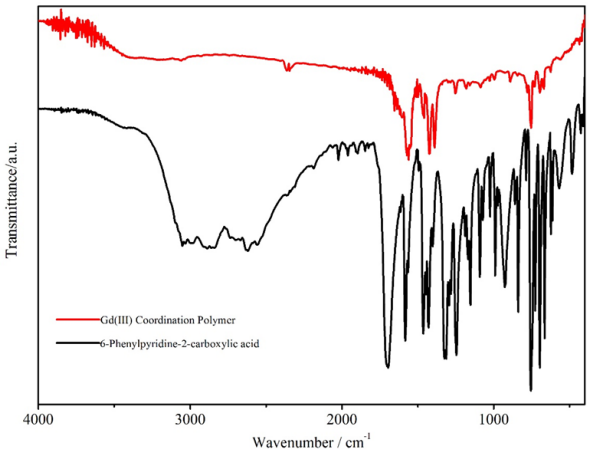

Figure 1. The infrared spectra of 6-phenylpyridine-2-carboxylic acid and the complex **1**.

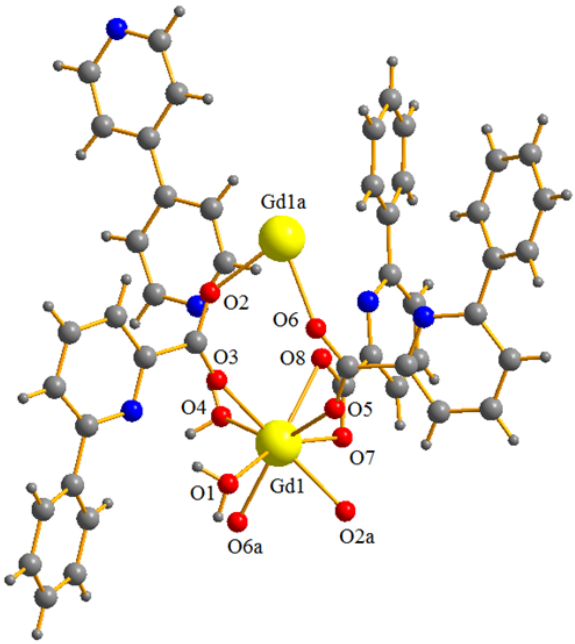

Figure 2. The molecular structure of $\{[Gd(L_1)_3(H_2O)_2]\cdot L_2\}_n$ (**1**).

2.3 Crystal Structure Determination

A single crystal of $\{[Gd(L_1)_3(H_2O)_2]\cdot L_2\}_n$ (**1**) (0.13 mm × 0.11 mm × 0.10 mm) was chosed for data collection on a SuperNova, Dual, Cu at zero, AtlasS2 four-circle diffractometer with graphite-monochromated Mo $K\alpha$ radiation (λ = 0.71073 Å) at 250.00 (10) K. The structure of **1** was solved and refined using SHELXT 2018/2 [32] and SHELXL 2017/1 [33], respectively. The absorption corrections were carried out using Olex2 [34]. The important crystal data of **1** are listed in Table 1.

2.4 Photocatalytic CO_2 Reduction Test

The photocatalytic CO_2 reduction reaction was performed according to the following steps: 0.05g of **1** and 100 mL H_2O were added into the quartz reactor, which was maintained at 20 °C with continuous stirring. And bubbling of high purity CO_2 gas for 15 min to fill the whole reactor. The used light source in the reaction was a 300 W Xe arc lamp (Beijing Trusttech Co., Ltd (PLS-SXE300). In the process of photocatalytic CO_2 reduction, gas samples were obtained every hour to analyze the product via a gas chromatograph equipped with Porapak Q column with FID detector.

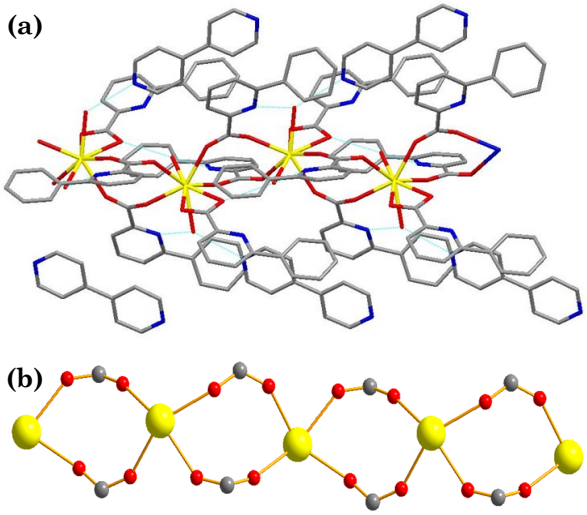

Figure 3. (a) 1D chain structure of $\{[Gd(L_1)_3(H_2O)_2]\cdot L_2\}_n$ (**1**), (b) 1D ring structure constructed by Gd(III) ions and bridging carboxylate groups.

3. Results and Discussion

3.1 Infrared Spectra

Figure 1 show the infrared spectra of 6-phenylpyridine-2-carboxylic acid and the complex **1**. In complex **1**, the bands at 1646 cm^{-1} and 1575 cm^{-1} are assigned to ($\nu_{as}(COO^-)$) and ($\nu_s(COO^-)$) of 6-phenylpyridine-2-carboxylic acid, respectively, the bands appear at 1571 ($\nu_{as}(COO^-)$) and 1423 ($\nu_s(COO^-)$) in complex **1**, indicating that the carboxylate of deprotonated 6-phenylpyridine-2-carboxylic acid ligand is coordinated with Gd(III) ion. which are consistent with the result of X-ray single-crystal diffraction analysis.

3.2 Structural Description of Complex 1

The molecular structure of $\{[Gd(L_1)_3(H_2O)_2]\cdot L_2\}_n$ (**1**) is shown in Figure 2. Selected bond lengths and angles of $\{[Gd(L_1)_3(H_2O)_2]\cdot L_2\}_n$ (**1**) are given in Table 2. The 1D chain of **1** is shown in Figure 3. The 3D network of **1** is shown in Figure 4. The hydrogen bond parameters are given in Table 3.

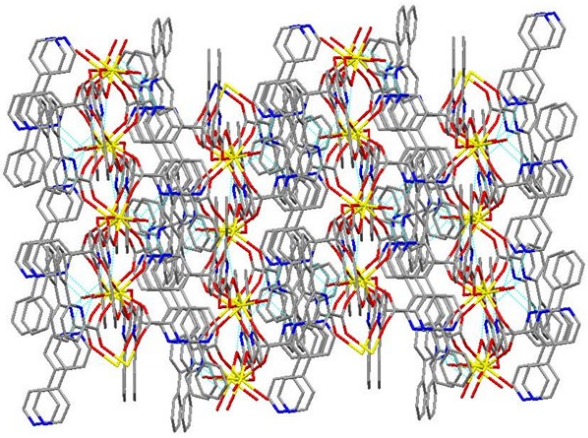

Figure 4. 3D network structure of $\{[Gd(L_1)_3(H_2O)_2]\cdot L_2\}_n$ (**1**).

Table 2. Selected bond lengths and angles of $\{[Gd(L_1)_3(H_2O)_2]\cdot L_2\}_n$ (**1**).

Bond	*d*	Angle	(°)
Gd1-O1	2.423(2)	O1-Gd1-O4	114.07(9)
Gd1-O2a	2.339(2)	O1-Gd1-O7	158.82(8)
Gd1-O3	2.304(2)	O1-Gd1-O8	146.83(8)
Gd1-O4	2.426(3)	O1-Gd1-O2a	86.12(8)
Gd1-O5	2.330(3)	O4-Gd1-O2a	135.75(9)
Gd1-O6a	2.349(2)	O2a-Gd1-O6a	77.85(8)
Gd1-O7	2.461(2)	O2a-Gd1-O7	75.16(9)
Gd1-O8	2.489(2)	O2a-Gd1-O8	111.01(8)
C13-O2	1.254(4)	O1-Gd1-O3	70.24(8)
C13-O3	1.240(4)	O3-Gd1-O2a	148.60(10)
C1-O5	1.251(4)	O3-Gd1-O4	74.54(10)
C1-O6	1.248(4)	O3-Gd1-O5	82.63(9)
C25-O7	1.259(4)	O3-Gd1-O6a	114.14(8)
C25-O8	1.257(4)	O3-Gd1-O7	130.76(8)
C14-N1	1.341(4)	O3-Gd1-O8	82.13(8)
C18-N1	1.344(4)	O4-Gd1-O7	74.94(10)
C2-N2	1.336(4)	O4-Gd1-O8	73.88(9)
C6-N2	1.341(5)	O1-Gd1-O5	83.48(10)
C26-N3	1.319(4)	O5-Gd1-O2a	74.17(8)
C30-N3	1.342(5)	O5-Gd1-O4	143.31(9)
		O5-Gd1-O6^i	146.11(9)
		O5-Gd1-O7	100.47(9)
		O5-Gd1-O8	74.86(9)
		O6a-Gd1-O1	75.85(9)
		O6a-Gd1-O4	70.49(9)
		O6a-Gd1-O7	90.36(9)
		O6a-Gd1-O8	134.15(9)
		O7-Gd1-O8	52.62(7)

Symmetry codes: (a) 3/2-*x*, -1/2+*y*,1/2-*z*.

Complex **1** is made up of one Gd(III) ions, three 6-phenylpyridine-2-carboxylate ligands, two coordinated water molecules and one uncoordinated 4,4'-bipyridine molecule. The Gd(III) ion in **1** is eight-coordinated and surrounded by six O atoms (O3, O5, O7, O8, O2a, O6a) from three 6-phenylpyridine-2-carboxylate ligands and two O atoms (O1, O4,) from two coordinated water molecules, respectively. In **1**, the carboxylate groups of 6-phenylpyridine-2-carboxylate ligands adopt bidentate chelating mode: one is two carboxyl oxygen atoms are coordinated with the same Gd (III) ion, and the other is two carboxyl oxygen atoms are coordinated with different Gd (III) ions. The nitrogen atom of 6-phenylpyridine-2-carboxylate ligand does not take part coordination with Gd (III) ion, so the coordination mode of 6-phenylpyridine-2-carboxylate ligands is different with ref. [23–31]. Which indicating oxygen atoms have a stronger coordination capacity with rare earth ions than nitrogen atom. The bond distances around Gd (III) are 2.423(2) Å (Gd1-O1), 2.339(2) Å (Gd1-O2a), 2.304(2) Å (Gd1-O3), 2.426(3) Å (Gd1-O4), 2.330(3) Å (Gd1-O5), 2.349(2) Å (Gd1-O6a), 2.461(2) Å (Gd1-O7), 2.489(2) Å (Gd1-O8), respectively, which consistent with other Gd (III) complexes [35,36]. The Gd (III) ions form eight member ring $Gd_2O_4C_2$ by the bridging effect of carboxylate groups, and the complex **1** forms 1D chain structure through eight member rings and intermolecular and intramolecular O−H···O and O−H···N hydrogen bonds (Figure 3 and Table 3) forming by O atoms of 6-phenylpyridine-2-carboxylate ligands, O atoms of coordinated water molecules and N atoms of 4,4'-bipyridine molecules. And the 1D chains further form a 3D network structure through hydrogen bond interactions and π-π interactions (Figure 4). Although 4,4'-bipyridine does not participate in coordination with Gd (III) ion, however, it is combined with one-dimensional chain through hydrogen bond interactions and plays an important role in stabilizing the complex molecule and three-dimensional network structure (Figure 5).

3.3 Photocatalytic CO_2 Reduction Studies

In order to explore the application of $\{[Gd(L_1)_3(H_2O)_2]\cdot L_2\}_n$ (**1**) in the field of photocatalytic CO_2 reduction, the photocatalytic CO_2 reduction test was carried out. As shown in Figure 6, the Gd (III) complex exhibits excel-

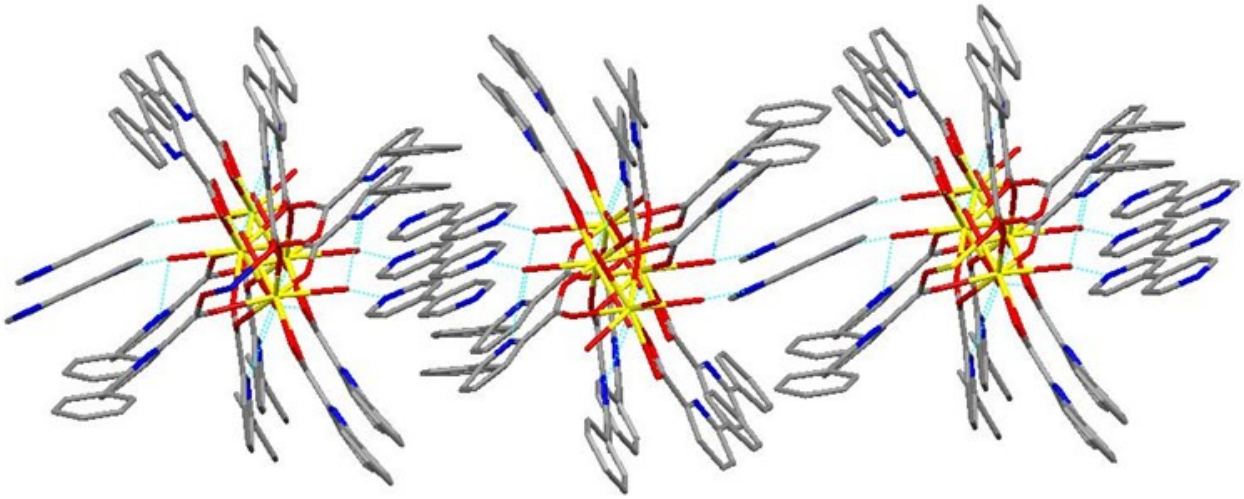

Figure 5. The hydrogen bond interactions of 4,4'-bipyridine.

Table 3. Hydrogen bond geometry of $\{[Gd(L_1)_3(H_2O)_2]\cdot L_2\}_n$ (**1**).

D−H···A	d(D−H) (Å)	d(H···A) (Å)	d(D−A) (Å)	∠DHA (°)
O1−H1A···O8^{i}	0.86	2.02	2.731(3)	140
O1−H1B···O3	0.86	2.42	2.722(3)	102
O1−H1B···N1	0.86	2.13	2.977(4)	168
O4−H4A···N2^{i}	0.86	2.08	2.910(5)	162
O4−H4B···N4^{ii}	0.81	2.05	2.861(5)	174

Symmetry codes: (i) 3/2-*x*, -1/2+*y*,1/2-*z*; (ii) *x*, *y*, *z*.

lent CO_2 reduction activity. With the increase of time, the yield of CO gradually increased (from 18.2 μmol/g in the first hour to 60.3 μmol/g in the third hour), indicating that the Gd(III) complex really possesses the catalytic capacity of CO_2. The yield of CO in this work is higher than those of g-C_3N_4 (1.8 mol.g^{-1}.h^{-1}) [37], Cu atom/g-C_3N_4 (3.1 mol.g^{-1}.h^{-1}) [37], BiOI (5.18 mol.g^{-1}.h^{-1}) [38], La-TiO_2 (3.5 mol.g^{-1}.h^{-1}) [39], Bi_2WO_6 (7.12 mol.g^{-1}.h^{-1}) [40], porphyrin MOF (6.882 mol.g^{-1}.h^{-1}) [41] and NH_2-MIL-125 (8.25 mol.g^{-1}.h^{-1}) [42], however, lower than those of TiO_{2-x}/g-C_3N_4 (77.8 mol.g^{-1}.h^{-1}) [43] and Yb(III) complex (48.7 mol.g^{-1}.h^{-1}) [44]. In additon, in the gas phase products, we only found CO products, no methane and other products detected because reducing CO_2 into CO only requires two electrons (CO_2 + 2H* + 2 e^- → CO + H_2O), while reducing CO_2 into CH_4 requires eight electrons (CO_2 + 8H* + 8e^- → CH_4 + 2H_2O). Therefore, it's harder to get methane products compared to CO.The CO selectivity has reached 100%, which is better than that of Yb(III) complex [44]. Such good selectivity is very favorable for future industrialization.

To confirm whether the complex **1** could maintain the photocatalytic CO_2 reduction peiformance, the CO_2 reduction test was circularly performed for three times. After each photocatalytic CO_2 reduction test, the reactor is opened with stirring to be fully exposed into the air. Subsequently, the second cyclic test was continued to perform according to the same method of photocatalytic CO_2 reduction. Similarly, the third loop test does the same. It can be obviously observed in Figure 7, the complex **1** displays similar photocatalytic CO_2 activity. The result indicates the photocatalytic activity of complex **1** is stability.

4. Conclusions

In summary, a new Gd(III) coordination polymer has been synthesized and structurally characterized. The photocatalytic CO_2 reduction activity shows that the complex **1** as catalyst exhibits excellent CO_2 reduction activity with the yield of CO from 18.2 μmol/g in the first hour to 60.3 μmol/g in the third hour. And the CO selectivity has reached 100%.

Acknowledgments

The authors would like to thank the National Natural Science Foundation of China (No.21171132), the Natural Science Foundation of Shandong (ZR2014BL003), the Project of Shandong Province Higher Educational Science and Technology Program (J14LC01), the Research Fund for the Doctoral Program of Weifang University (NO. 2021BS09), the Science Foundation of Weifang, and Science Foundation of Weiyuan Scholars Innovation Team.

CRediT Author Statement

Author Contributions: Xi-Shi Tai and Xi-Hai Yan: Conceptualization, Methodology, Investigation, Resources, Data Curation, Writing, Review. Yuan-Fang Wang and Li-Hua Wang: Investigation, Resources, Writing, Review and Editing, Validation. All authors have read and agreed to the published version of the manuscript.

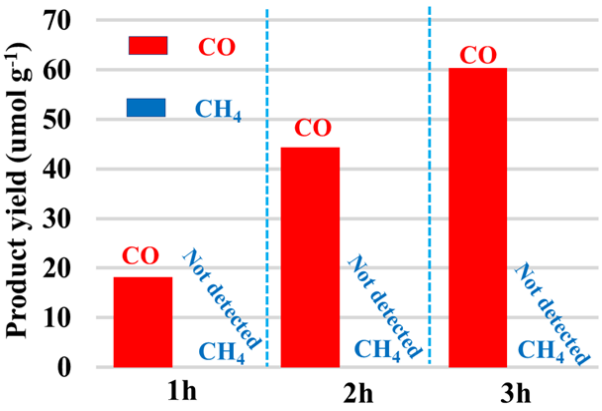

Figure 6. The comparison CO_2 photoconversion activity of {[Gd(L$_1$)$_3$(H$_2$O)$_2$]·L$_2$}$_n$ (**1**) under UV-vis light irradiation.

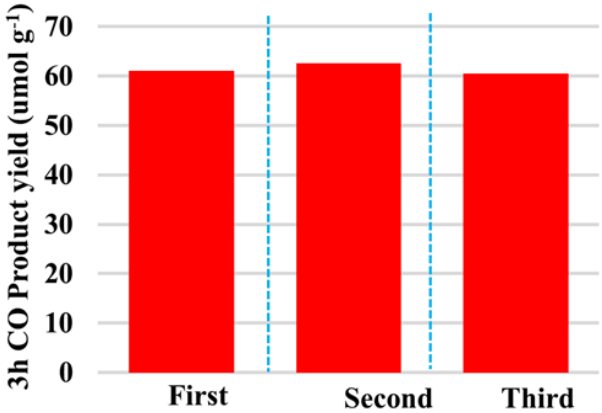

Figure 7. Repeated photocatalytic CO_2 reduction activity over complex **1** as the photocatalyst for three times.

References

[1] Zhou, J., Yu, W.T., Tang, S.S., He, X.M., Zhang, X.L., Zhou, L., Sun, L., Zhang, J. (2022). Tuning the bonding dimensions for coordination polymers based on rare earth metal ions. *Chinese Journal of Structural Chemistry*, 24, 7500-7504. DOI: 10.1039/d2ce01131j.

[2] Calado, C.M.S., da Silva, K.R.M., Santos, T.V., Viana, R.D., Meneghetti, S.M.P., Barbosa, C.D.D.S. (2022). Green and facile synthesis of EuBDC coordination polymer: Effects of ultrasound and stabilizing agent on morphological, structural and photophysical properties. *Optical Materials*, 125, 112107. DOI: 10.1016/j.optmat.2022.112107.

[3] Wang, L., Liu, H., Huang, S., Zhong, S.L. (2021). Low-temperature molten salt synthesis and luminescence properties of Eu(III)-based coordination polymer nanosheets. *Rare Metals*, 40, 728-735. DOI: 10.1007/s12598-017-0914-9.

[4] Khalfaoui, O., Beghidja, A., Beghidja, C., Guari, Y., Larionova, J., Long, J. (2021). Synthesis, crystal structures, luminescent and magnetic properties of rare earth dinuclear complexes and one-dimensional coordination polymers supported by two derivatives of cinnamic acid. *Polyhedron*, 207, 115366. DOI: 10.1016/j.poly.2021.115366.

[5] Liu, M.C., Yin, Q.Q., Zhong, S.N., Sun, H.M., Wang, Y.B., Liu, S., Wang, J., Diao, Y.Y., Yang, F.F., Xin, T.T. (2022). Two novel rare earth coordination polymers derived from zwitterionic 1,3-bis(1-carboxylatoethyl)imidazolium bromide: structures and magnetic properties. *Journal of Molecular Structure*, 1250, 131665. DOI: 10.1016/j.molstruc.2021.131665.

[6] Yang, L.Z., Yang, R.X., Zhu, P.Y., Yue, T.C., Yu, Y.M., Wang, D.Z., Wang, L.L. (2023). Magnetic, fluorescence and electric properties of rare earth complexes based on reduced Schiff base carboxylic acid ligand. *Journal of Molecular Structure*, 1281, 135177. DOI: 10.1016/j.molstruc.2023.135177.

[7] Zeng, Z.J., Shen, H.X., Gao, W., Guo, Q.F., Chen, M.J., Yan, X.J., Liu, H.N. Ji, Y.H. (2022). A novel biocompatible Eu-based coordination polymers of cytarabine anticancer drug: Preparation, luminescence properties and in vitro anticancer activity studies. *Frontiers in Chemistry*, 10, 1043810. DOI: 10.3389/fchem.2022.1043810.

[8] Zhang, L.Y., Shi, H.R., Tan, X., Jiang, Z.Q., Wang, P., Qin, J.L. (2022). Ten-gram-scale mechanochemical synthesis of ternary lanthanum coordination polymers for antibacterial and antitumor activities. *Frontiers in Chemistry*, 10, 898324. DOI: 10.3389/fchem.2022.898324.

[9] Xue, D.X., Cairns, A.J., Belmabkhout, Y., Wojtas, L., Liu, Y.L., Alkordi, M.H., Eddaoudi, M. (2013). Tunable rare-earth fcu-MOFs: a platform for systematic enhancement of CO_2 adsorption energetics and uptake. *Journal of the American Chemical Society*, 135, 7660-7667. DOI: 10.1021/ja401429x.

[10] Meng, S.Y., Li, G., Wang, P., He, M., Sun, X.H., Li, Z.X. (2023). Rare earth-based MOFs for photo/electrocatalysis. *Materials Chemistry Frontiers*, 5, 806-827. DOI: 10.1039/D2QM01201D.

[11] Sinchow, M., Semakul, N., Konno, T., Rujiwatra, A. (2021). Lanthanide coordination polymers through design for exceptional catalytic performances in CO_2 cycloaddition reactions. *ACS Sustainable Chemistry & Engineering*, 9, 8581-8591. DOI: 10.1021/acssuschemeng.1c01955.

[12] Shen, T., Ni, X.F., Ling, J. (2021). Recent progress in ring-opening polymerizations catalyzed by rare earth catalysts. *Acta Polymerica Sinica*, 52, 445-455. DOI: 10.11777/j.issn1000-3304.2020.20261.

[13] Li, X.L., Xu, T.Q. (2023). Stereoselective polymerization of aromatic vinyl polar monomers. *European Journal of Inorganic Chemistry*, 26, e202200699. DOI: 10.1002/ejic.202200699.

[14] Wang, H.H., Cue, J.M.O., Calubaquib, E.L., Kularatne, R.N., Taslimy, S., Miller, J.T., Stefan, M.C. (2021). Neodymium catalysts for polymerization of dienes, vinyl monomers, and epsilon-caprolactone. *Polymer Chemistry*, 12, 6790-6823. DOI: 10.1039/d1py01270c.

[15] Skvortsov, G.G., Shavyrin, A.S., Kovylina, T.A., Cherkasov, A.V., Trifonov, A.A. (2019). Rare-earth amido and borohydrido complexes supported by tetradentate amidinate ligands: synthesis, structure, and catalytic activity in polymerization of cyclic esters. *European Journal of Inorganic Chemistry*, 2019, 5008-5017. DOI: 10.1002/ejic.201900897.

[16] Fu, J.W., Jiang, K.X., Qiu, X.Q., Yu, J.G., Liu, M. (2020). Product selectivity of photocatalytic CO_2 reduction reactions. *Materials Today*, 32, 222-243. DOI: 10.1016/j.mattod.2019.06.009.

[17] Kamakura, Y., Suppaso, C., Yamamoto, I., Mizuochi, R., Asai, Y., Motohashi, T., Tanaka, D., Maeda, K. (2023). Tin(II)-based metal-organic frameworks enabling efficient, selective reduction of CO_2 to formate under visible light. *Angewandte Chemie - International Edition*, 62, e202305923. DOI: 10.1002/anie.202305923.

[18] Zhang, J.H., Wang, Y.C., Wang, H.J., Zhong, D.C., Lu, T.B. (2022). Enhancing photocatalytic performance of metal-organic frameworks for CO2 reduction by a bimetallic strategy. *Chinese Chemical Letters*, 33, 2065-2068. DOI: 10.1016/j.cclet.2021.09.035.

[19] Liu, D.C., Zhang, M.L., Huang, H.H., Feng, Q., Su, C., Mo, A.N., Wang, J.W., Qi, Z.P., Zhang, X.J., Jiang, L., Chen, Z.L. (2021). Co-II-Zn-II heterometallic dinuclear complex with enhanced photocatalytic activity for CO_2-to-CO conversion in a water-containing system. *ACS Sustainable Chemistry & Engineering*, 9, 9273-9281. DOI: 10.1021/acssuschemeng.1c01708.

[20] Huang, N.Y., He, H., Liu, S.J., Zhu, H.L., Li, Y.J., Xu, J., Huang, J.R., Wang, X., Liao, P.Q., Chen, X.M. (2021). Electrostatic attraction-driven assembly of a metal-organic framework with a photosensitizer boosts photocatalytic CO_2 reduction to CO. *Journal of the American Chemical Society*, 143, 17424-17430. DOI: 10.1021/jacs.1c05839.

[21] Dong, Y.L., Liu, H.R., Wang, S.M., Guan, G.W., Yang, Q.Y. (2023). Immobilizing isatin-schiff base complexes in NH_2-UiO-66 for highly photocatalytic CO_2 reduction. *ACS Catalysis*, 13, 2547-2554. DOI: 10.1021/acscatal.2c04588

[22] Kumagai, H., Tamaki, Y., Ishitani, O. (2022). Photocatalytic systems for CO_2 reduction: metal-complex photocatalysts and their hybrids with photofunctional solid materials. *Accounts of Chemical Research*, 55, 978-990. DOI: 10.1021/acs.accounts.1c00705.

[23] Wang, L.H., Kong, F.Y., Tai, X.S. (2022). Synthesis, crystal structure and catalytic activity of tri-nuclear Zn(II) complex based on 6-phenylpyridine-2-carboxylic acid and bis(4-pyridyl)amine ligands. *Bulletin of Chemical Reaction Engineering & Catalysis*, 17, 394-402. DOI: 10.9767/bcrec.17.2.13952.394-402.

[24] Tai, X.S., Xia, Y.P. (2022). The Crystal Structure of [(2,2'-Bipyridine-κ² N,N)-bis(6-phenylpyridine-2-carboxylato-κ² *N,O*)cobalt(II)]-monohydrate, $C_{36}H_{26}N_4O_5Co$. *Zeitschrift für Kristallographie. New Crystal Structures,* 237, 225-227. DOI: 10.1515/ncrs-2021-0473.

[25] Tai, X.S., Liang, L., Li, X.T., Cao, S.H., Wang, L.H. (2021). Crystal Structure of Diaqua-bis(μ²-6-phenylpyridine-2-carboxylate-κ³*N,O:O*)-bis(6-phenylpyridine-2-carboxylato-κ²*N,O*)lead(II)-N,N-dimethylformamide-water (1/2/4), $C_{54}H_{58}N_6O_{16}Pb_2$. *Zeitschrift für Kristallographie. New Crystal Structures,* 236, 1199-1201. DOI: 10.1515/ncrs-2021-0277.

[26] Tai, X.S., Wang, Z.J., Ouyang, J., Li, Y.F., Zhang, W., Jia, W.L., Wang, L.H. (2021). The Crystal Structure of [(Phenantroline-κ²*N,N*')-bis(6-phenylpyridine-2-carboxylate-κ² *N,O*)cobalt(II)]monohydrate, $C_{36}H_{26}N_4O_5Co$. *Zeitschrift für Kristallographie. New Crystal Structures,* 236, 1309-1311. DOI: 10.1515/ncrs-2021-0319.

[27] Wang, L.H., Tai, X.S., Xia, Y.P. (2022). The Crystal Structure of *Catena-poly*[(m²-4,4′-bipyridine-κ²*N:N*)-bis(6-phenylpyridine-2-carboxylato-κ²*N,O*) zinc(II)], $C_{34}H_{24}N_4O_4Zn$. *Zeitschrift für Kristallographie. New Crystal Structures,* 237, 305-307. DOI: 10.1515/ncrs-2022-0003.

[28] Feng, Y.M., Tai, X.S., Xia, Y.P. (2022). The crystal structure of [(2,2'-bipyridine-κ²*N,N*)-bis(6-phenylpyridine-2-carboxylate-κ²*N,O*)copper(II)], $C_{34}H_{24}N_4O_4Cu$. *Zeitschrift für Kristallographie. New Crystal Structures,* 237, 285-287. DOI: 10.1515/ncrs-2021-0486.

[29] Liu, P., Wang, L.H., Tai, X.S. (2023). The crystal structure of *catena*-poly[bis(6-phenylpyridine-2-carboxylato-κ²N,O)-(μ 2-4,4′-bipyridne-κ² *N*:*N*)cadmium(II)], $C_{34}H_{24}N_4O_4Cd$. *Zeitschrift für Kristallographie. New Crystal Structures,* 238, 771-773. DOI: 10.1515/ncrs-2023-0201.

[30] Wang, L.H., Kong, F.Y., Tai, X.S. (2022). Synthesis, structural characterization of a new Ni(II) complex and its catalytic activity for oxidation of benzyl alcohol. *Bulletin of Chemical Reaction Engineering & Catalysis*, 17, 375-382. DOI: 10.9767/bcrec.17.2.13975.375-382.

[31] Wang, L.H., Tai, X.S. (2022). The crystal structure of diaqua-bis(6-phenylpyridine-2-carboxylato-κ²N,O)manganese(II)-water-dimethylformamide(1/2/1), $C_{27}H_{31}N_3O_9Mn$. *Zeitschrift für Kristallographie. New Crystal Structures,* 237, 675-677. DOI: 10.1515/ncrs-2022-0119.

[32] Sheldrick, G.M. (2015). Crystal Structure Refinement with SHELXL. *Acta Crystallographica*, C71, 3-8. DOI: 10.1107/S2053229614024218.

[33] Sheldrick, G.M. (2015). *SHELXT*-Integrated space-group and crystal-structure determination. *Acta Crystallographica*, A71, 3-8. DOI: 10.1107/S2053273314026370.

[34] Dolomanov, O.V., Bourhis, L.J., Gildea, R.J., Howard, J.A.K., Puschmann, H. (2009). OLEX2: A Complete Structure Solution, Refinement and Analysis Program. *Journal of Applied Crystallography*, 42, 339-341. DOI: 10.1107/S0021889808042726.

[35] Niu, S.Y., Jin, J., Jin, X.L., Cong, Y., Yang, Z.Z. (2000). Crystal structure and magnetism of the binuclear Gd(III) complex $Gd_2(C_{12}H_8N_2)_2(C_6H_5COO)_6$. *Chinese Science Bulletin*, 45, 706-711. DOI: 10.1007/BF02886174.

[36] Li, W.J., Chen, W.Z., Huang, M.L. (2016). Synthesis and crystal stucture of the mixed complex $[Gd(Ts\text{-}p\text{-}aba)_3(phen)]_2.2DMF.4.4H_2O$. *Journal of Synthetic Crystals*, 45, 2113-2117. DOI: 10.16553/j.cnki.issn1000-985x.2016.08.022.

[37] Li, Y., Li, B.H., Zhang, D.N., Cheng, L., Xiang, Q.J. (2020). Crystalline carbon nitride supported copper single atoms for photocatalytic CO_2 reduction with nearly 100% CO selectivity. *ACS Nano*, 14, 10552-10561. DOI: 10.1021/acsnano.0c04544.

[38] Ye, L.Q., Jin, X.L., Ji, X.B., Liu, C., Su, Y.R., Xie, H.Q., Liu, C. (2016). Facet-dependent photocatalytic reduction of CO_2 on BiOI nanosheets. *Chemical Engineering Journal*, 291, 39-46. DOI: 10.1016/j.cej.2016.01.032.

[39] Liu, Y., Zhou, S., Li, J., Wang, Y., Jiang, G., Zhao, Z., Liu, B., Gong, X., Duan, A., Liu, J., Wei, Y., Zhang, L. (2015). Photocatalytic reduction of CO_2 with water vapor on surface La-modified TiO_2 nanoparticles with enhanced CH_4 selectivity. *Applied Catalysis B: Environmental*, 168-169, 125-131. DOI: 10.1016/j.apcatb.2014.12.011.

[40] Liu, Y.P., Shen, D.Y., Zhang, Q., Lin, Y., Peng, F. (2021). Enhanced photocatalytic CO_2 reduction in H_2O vapor by atomically thin Bi_2WO_6 nanosheets with hydrophobic and nonpolar surface. *Applied Catalysis B: Environmental*, 283, 119630. DOI: 10.1016/j.apcatb.2020.119630.

[41] Zheng, C., Qiu, X.Y., Han, J.Y., Wu, Y.F., Liu, S.Q. (2019). Zero-dimensional-g-CNQD-coordinated two-dimensional porphyrin MOF hybrids for boosting photocatalytic CO_2 reduction. *ACS Applied Materials & Interfaces*, 45, 42243-42249. DOI: 10.1021/acsami.9b15306.

[42] Cheng, X.M., Dao, X.Y., Wang, S.Q., Zhao, J., Sun, W.Y. (2021). Enhanced photocatalytic CO_2 reduction activity over NH_2-MIL-125(Ti) by facet regulation. *ACS Catalysis*, 11, 650-658. DOI: 10.1021/acscatal.0c04426.

[43] Shi, H., Long, S., Hu, S., Hou, J., Ni, W., Song, C., Li, K., Gurzadyan, G.G., Guo, X. (2019). Interfacial charge transfer in 0D/2D defect-rich heterostructures for efficient solar-driven CO_2 reduction. *Applied Catalysis B: Environmental*, 245, 760-769. DOI: 10.1016/j.apcatb.2019.01.036.

[44] Tai, X.S., Wang, Y.F., Wang, L.H., Yan, X.H. (2023). Synthesis, structural characterization, Hirschfeld surface analysis and photocatalytic CO_2 reduction of Yb(III) complex with 4-aacetylphenoxyacetic acid and 1,10-phenanthroline ligands. *Bulletin of Chemical Reaction Engineering & Catalysis*, 18, 285-293. DOI: 10.9767/bcrec.18471.